Environ Sci Pollut Res (2015) 22:11057–11066
DOI 10.1007/s11356-015-4355-4

RESEARCH ARTICLE

Cytotoxicity of aluminum oxide nanoparticles on *Allium cepa* root tip—effects of oxidative stress generation and biouptake

A. Rajeshwari[1] · S. Kavitha[1] · Sruthi Ann Alex[1] · Deepak Kumar[1] · Anita Mukherjee[2] · Natarajan Chandrasekaran[1] · Amitava Mukherjee[1]

Received: 20 January 2015 / Accepted: 9 March 2015 / Published online: 21 March 2015

Abstract The commercial usage of Al_2O_3 nanoparticles (Al_2O_3 NPs) has gone up significantly in the recent times, enhancing the risk of environmental contamination with these agents and their consequent adverse effects on living systems. The current study has been designed to evaluate the cytogenetic potential of Al_2O_3 NPs in *Allium cepa* (root tip cells) at a range of exposure concentrations (0.01, 0.1, 1, 10, and 100 μg/mL), their uptake/internalization profile, and the oxidative stress generated. We noted a dose-dependent decrease in the mitotic index (42 to 28 %) and an increase in the number of chromosomal aberrations. Various chromosomal aberrations, e.g. sticky, multipolar and laggard chromosomes, chromosomal breaks, and the formation of binucleate cells, were observed by optical, fluorescence, and confocal laser scanning microscopy. FT-IR analysis demonstrated the surface chemical interaction between the nanoparticles and root tip cells. The biouptake of Al_2O_3 in particulate form led to reactive oxygen species generation, which in turn probably contributed to the induction of chromosomal aberrations.

Keywords Al_2O_3 NPs · *Allium cepa* · Aberration · Biouptake · SOD

Responsible editor: Elena Maestri

Dr. Amitava Mukherjee, Sr. Professor & Deputy Director, Centre for Nanobiotechnology, VIT University, and holds a BE, ME, Ph.D.

✉ Amitava Mukherjee
amit.mookerjea@gmail.com; amitav@vit.ac.in

[1] Centre for Nanobiotechnology, VIT University, Vellore, India

[2] Centre of Advanced Study, Department of Botany, University of Calcutta, Kolkata, India

Introduction

In the past decades, engineered nanoparticles have been developed extensively, and they have gained wide recognition in variety of commercial and industrial applications. According to the market survey, the production of metal oxide nanoparticles was estimated to rise from 2,70,041 tons in 2012 to 16, 63,168 tons by 2020, and among these nanoparticles, aluminum oxide nanoparticles (Al_2O_3 NPs) are one of the most abundantly used engineered nanoparticles (Yang et al. 2012; Future Markets Inc. 2013). Due to their dielectric and abrasive properties, Al_2O_3 NPs have been used as an abrasive agent and insulators (Prabhakar et al. 2012). Al_2O_3 NPs are widely being used in various applications, including alloys, explosives, rocket fuel, wear-resistant coatings for ships, energetics, sensors, personal care products, and drug delivery systems (Darlington et al. 2009; Jiang et al. 2009; Schrand et al. 2010; Sadiq et al. 2011). These nanometer-sized materials also have enhanced toxicity in comparison to bulk material when unleashed into the environment (Donaldson et al. 2001). Al_2O_3 NPs were found to appreciably induce toxicity by increasing the frequency of micronucleus occurrence, chromosomal losses, mutations, and polyploidy (Di Virgilio et al. 2010). The minimal reports on their toxicity and genotoxicity in spite of their increased use in industries have inspired the toxicity evaluation of Al_2O_3 NPs, in particular (Tsaousi et al. 2010).

Nanoparticles can have positive and negative impacts on higher plants and their consumers in the food chain (Rico et al. 2011). Al_2O_3 NPs with varying diameters and surface compositions can be engineered for evading the reticuloendothelial system (Faraji and Wipf 2009) or can be complexed with antibodies to attain targeted drug delivery (Arruebo et al. 2009). These ceramic nanoparticles are also known to be beneficial as they possess antimicrobial properties, which result

due to the electrostatic attraction between their positive surface and the negatively charged bacteria, thus decreasing the viability of microbes (Mukherjee et al. 2011). In addition, their high surface reactivity is known to cause increased risk of the nanoparticles being entrapped in the gill mucus of marine organisms, and thereby hinder respiratory processes and transportation of ions (Baker et al. 2014). In mammalian systems, they can decrease the tight junction protein expression, alter the properties of the blood-brain barrier, and induce toxicity to the microvascular endothelium (Chen et al. 2008). Hence, it is highly mandatory to study the toxicity profile of Al_2O_3 NPs. For studies concerning the mutagenesis in higher eukaryotes, plants have generally been used as a test system in order to study the effect of nanoparticles (Fiskesjo 1985). Al_2O_3 NP exposure are known to cause the rapid depolarization of plasma membrane, which was more extensive in the distal cellular portions, and the extent was influenced by the developmental state of cells (Illéš et al. 2006). Al_2O_3 NP toxicity can also lead to the inhibition of basipetal polar transport of auxin in the outer cortex cells and epidermis (Hasenstein and Evans 1988). The foremost uncertainty with regard to Al_2O_3 NP phytotoxicity is the primary route of action at the subcellular level; however, the root apex has been cited as the primary injury site by Ryan et al. (1993).

The easily distinguishable genetic endpoints, including chromosomal aberrations, alterations in ploidy, and sister chromatid exchanges, have made the plant system ideal for studies (Kumari et al. 2011). In addition, the *Allium cepa* root chromosomal aberration assay has been authenticated by the United Nations Environment Programme (UNEP) (Grant 1982) and the International Programme on Chemical Safety (IPCS) (WHO 1985) as an effective conventional plant bioassay and as an established standard test for the in situ monitoring of environmental substances and chemical screening (Cabrera and Rodriguez 1999). Chromosomal aberrations have been determined by using *A. cepa* since 1920s (Satapathy and Swamy 2013; Kanaya et al. 1994). The clear mitotic phases, stable chromosome number and karyotype, diversity of chromosome morphology, rapid response to genotoxic materials, and the rare occurrences of spontaneous chromosomal damages are the features that make *A. cepa* an excellent plant system for studying the toxicity of nanoparticles (Firbas and Amon 2013). For genotoxicity screening during cell division or microspore formation, root tips are shown to be convenient for microscopic analysis of features like mitotic or meiotic aberrations, respectively (Kristen 1997).

Kumari et al. (2009) have used the *A. cepa* as an indicator to evaluate the genotoxic effect of AgNPs. Cell damages in *A. cepa* were observed by Chen et al. (2010) in the presence of carbon nanoparticles for a range of exposure concentrations from 10 to 110 mg/L. The role of ROS in causing genotoxicity in *A. cepa* by ZnO and AgNPs was later on reported by Panda et al. (2011) and Kumari et al. (2011), respectively. Similarly, Ghodake et al. (2011) have assessed the phytotoxic nature of cobalt and zinc oxide nanoparticles in *A. cepa*. Liman (2013) also used *A. cepa* as a test system to evaluate the genotoxic effect of bismuth (III) oxide nanoparticles. Recently, Pakrashi et al. (2014) have reported the toxic effect of TiO_2 NPs on *A. cepa* by studying their internalization and ROS generation. However, there have been just a handful reports that explore the phytotoxicity of Al_2O_3 NPs. It has been reported by Kim et al. (2009) that Al_2O_3 NPs could affect cultured mammalian cells by inducing cytotoxicity and primary DNA damage; however, no mutagens were observed by them.

Thus, the current toxicity study is the first of its nature to evaluate the cytogenetic effect of Al_2O_3 NPs in *A. cepa*. The various chromosomal aberrations were observed by optical, fluorescence, and confocal laser microscopy for a wide range of Al_2O_3 NP concentrations (0.01, 0.1, 1, 10, 100 μg/mL). This also happens to be the first study that evaluates the cytogenetic effect of nanomaterials using *A. cepa* model at exposure concentrations ≤1 μg/mL. The cytotoxicity of Al_2O_3 NPs on *A. cepa* root tip cells was evaluated by tracking the changes in the mitotic index and chromosomal aberrations. Further, the dose-dependent toxicity was substantiated with the help of surface chemical analysis by FT-IR, internalization/uptake analyses by ICP-OES, and the antioxidant enzyme (SOD) assay.

Materials and methods

Chemicals

Aluminum oxide nanoparticles (γ-phase Al_2O_3 nanopowder, particle size <50 nm; CAS No. 1344-28-1) were procured from Sigma-Aldrich, USA. Acetocarmine, Acridine Orange (AO) dyes, Nitro Blue Tetrazolium (NBT), Riboflavin, and Ethylene diamine tetraacetic acid (EDTA) were obtained from HiMedia Labs, India.

Nanoparticle suspension preparation and characterization

The stock solution of Al_2O_3 NPs (200 μg/mL) was prepared by dispersing the NPs in Milli-Q water, and then, the solution was subjected to ultrasonic vibration for 30 min at 130 W to yield various concentrations of NP dispersions, 0.01, 0.1, 1, 10, and 100 μg/mL. These NP dispersions were used further for the interaction studies. The size distribution of Al_2O_3 NPs in Milli-Q water was analyzed by particle size analyzer (NanoBrook 90Plus Particle Size Analyzer). Approximately, 3 mL of NP dispersions were subjected to this analysis, and their particle sizes were determined by calculating the mean hydrodynamic diameter from the intensity of light scattered by the particles undergoing Brownian motion. The zeta potential

of Al_2O_3 NP dispersion was analyzed by Nano Partica (Nano Particle Analyzer, SZ-100, Horiba Scientific, Japan) in order to determine the surface charge of nanoparticles.

Test system and treatment

Three healthy onion bulbs (30–35 g each) were grown under dark conditions in an enclosed chamber. A temperature of 28± 2 °C was maintained, and renewed water supply was provided for every 24 h. Roots of 2 to 3-cm length were treated for 4 h with different concentrations of Al_2O_3 NPs (0.01, 0.1, 1, 10, and 100 μg/mL). For each concentration, three replicates were made for statistical validation of the observations.

Microscopic analysis

Optical microscopy

After 4-h interaction of root tips with various concentrations of Al_2O_3 NPs, the root tips were removed and rinsed with distilled deionized water. The acetocarmine squash technique was used for the microscopic analysis (Pakrashi et al. 2014). The rinsed root tips were placed in 1 N HCl for 10 min at 28 °C and then dipped in 1 % acetocarmine stain for 10 min. After the 10-min incubation, 1–2 mm of the roots were cut from the tip and placed over a glass slide, covered with a cover slip, and were pressed firmly with the help of a thumb to prepare a uniform squash. The slides were observed by an optical microscope (Axiostar, Zeiss, Germany) to view any cytological changes at ×1000 magnification.

Fluorescence microscopy

Interaction of the onion root tips with the Al_2O_3 NP dispersion with a minimum concentration of 0.01 μg/mL and a maximum of 100 μg/mL along with a control were carried out for 4 h. The root tips were then taken out, rinsed with deionized water, and incubated in 1 N HCl solution for 5–6 min at room temperature. The root tips were then stained with Acridine Orange (AO), a stain specific to the nucleus, for visualization of chromosomal aberrations. The root tips were dipped in Milli-Q water to remove any excess stain. The stained root tips of 2-mm length were placed over a glass slide, covered with a cover slip, and were pressed firmly with the support of a thumb to prepare a uniform squash of the root tips. Throughout the experiment, dark condition was retained to avoid photobleaching of dyes. The slides were analyzed at ×1000 magnification for cytological changes and chromosomal aberrations. Observation of fluorescence images was performed with the BP 450–490, LP 590 filter using a fluorescence microscope (DM-2500, Leica, Germany). The attached camera component (Leica-DFC-29) was used to record the images, and the image processing was carried out using Leica-Application Suite 3.8 (Pakrashi et al. 2014).

Confocal laser scanning microscopy

Interactions of the onion root tips were carried out with the Al_2O_3 NPs of minimum 0.01 μg/mL and a maximum 100 μg/mL concentration along with a control dispersion for 4 h. The root tips were then taken out and incubated for 5–6 min in the presence of 1 N HCl at room temperature. Then, the root tips were stained with 1 mL of AO, a nuclear-specific stain, for 15 min under dark conditions to prevent photobleaching of dyes. After centrifuging the suspensions at 6000 rpm, 0 °C for 15 min, the supernatant was discarded, and the roots were washed with Milli-Q water to remove the unbound dye. The root tips were placed over a glass slide, covered with a cover slip, and were pressed firmly with the help of a thumb to prepare a uniform squash. Analysis of the slides was done at ×1000 magnification for observing the cytological changes and chromosomal aberrations using a confocal laser scanning microscope (Zeiss Lsm 510 Meta), and the images were processed by LSM 5 Image Browser (Pakrashi et al. 2014).

Data analysis

To determine the toxic effect of Al_2O_3 NPs on *A. cepa* root tip cells, 1000 cells were scored per test concentration. The mitotic index and phase index based on the chromosomal aberration and different mitosis phases can be calculated as follows (Bakare et al. 2000; Fiskesjo 1997):

$$\text{Mitotic index}(\text{MI}\%) = \frac{T_{DC}}{T_C} \times 100 \quad (1)$$

$$\text{Phase index}(\text{PI}\%) = \frac{T_C}{T_{DC}} \times 100 \quad (2)$$

T_C Total number of cells observed
T_{DC} Total number of dividing cells

Internalization of NPs

To estimate the amount of NPs internalized into *A. cepa*, the roots were allowed to dry at 60 °C for 24 h following the 4-h interaction with NPs. The dried roots were powdered by using a mortar and pestle. The powdered samples were acid digested using concentrated HNO_3, and then, the soluble parts were filtered through 0.45-μm and 3-kDa membrane filter. The filtered samples were analyzed with the aid of inductive coupled plasma-optical emission spectroscopy (ICP-OES; Perkin Elmer Optima 5300 DV, USA) to determine the concentration of NPs internalized into the root cells.

Superoxide dismutase assay

To evaluate the SOD activity of the cells, 0.2 g of root tips was interacted with 0.01, 1, and 100 μg/mL of Al_2O_3 NP dispersion for 4 h. After the treatment, the root tips were crushed by using mortar and pestle by adding prechilled 1× PBS buffer, and the final volume was made up to 5 mL by adding 1× PBS buffer. The solutions were transferred to fresh falcon tubes, after which centrifugation was done for 10 min at 10,000 rpm. A total of 0.1 mL of the supernatants were transferred to fresh 2-mL centrifuge tubes, and 0.2 mL of 0.1 M of ethylene diamine tetraacetic acid (EDTA) and 0.1 mL of 1.5 mM nitrobluetetrazolium (NBT) prepared in PBS (pH 7.8) were added to these tubes. To these solutions, 50 μL of 10 μM riboflavin solution was added and incubated for 15 min under dark condition. After the 15-min incubation, the cell solutions were analyzed for SOD generation using the ELISA microplate reader at 560 nm.

Fourier transformer infrared spectroscopy analysis (FT-IR)

For FT-IR analysis, hot-air oven-drying of the 4-h interacted root tips in 100 μg/mL of Al_2O_3 NP dispersion along with the control root cells at 60 °C for 15 h was required. Then, the roots were subjected to FT-IR (IR Affinity1, Shimadzu) analysis in ATR mode.

Statistical analysis

The significance of the difference between Al_2O_3 NP-treated and control group was tested by one-way analysis of variance (ANOVA). All data were represented as arithmetic mean± standard error. The level of significance for all the results was accepted at $p<0.05$.

Results and discussion

Characterization of Al_2O_3 NPs

The aggregation behavior of nanoparticles in the test environment is considered as an important property for determining their toxic effect (Sayes and Warheit 2009). In order to analyze the stability and aggregation behavior of Al_2O_3 NPs, the mean hydrodynamic sizes of five test concentrations of Al_2O_3 NP (0.01, 0.1, 1, 10, and 100 μg/mL) dispersion in Milli-Q water were determined at 0 and 4 h, and the data are presented as Table 1 for better understanding. These results confirmed the uniform distribution of nanoparticles, and the insignificant differences in the particle sizes measured at 0 and 4 h in Milli-Q water could be attributed to the fact that the dispersions were stable during the exposure period. The agglomeration of the NPs was prevented by the electrostatic repulsion between NPs, which is responsible for the colloidal stability of nanoparticles. The zeta potential of Al_2O_3 NP dispersion in Milli-Q water was found to be 47±0.5 mV.

Table 1 The mean hydrodynamic diameter of Al_2O_3 NP dispersion during the experimental condition

Concentration of Al_2O_3 NPs (μg/mL)	Mean hydrodynamic diameter (nm)	
	At 0 h	At 4 h
0.01	150.90±1.50	126.20±1.40
0.1	169.20±12.00	168.60±4.10
1	160.80±3.90	123.40±4.60
10	154.00±11.00	123.40±6.10
100	142.40±8.00	142.40±3.10

Microscopic analysis

Optical microscopy

Plant test systems have been often employed as genetic models for monitoring and screening the environmental pollutants (Fiskesjo 1985). Optical microscopy gave a comprehensive view of the Al_2O_3 NP impacts. Table 2 shows the data indicating the mitotic and phase indices when *A. cepa* root tip cells were exposed to Al_2O_3 NPs at various concentrations ranging from 0.01, 0.1, 1, 10, and 100 μg/mL after 4-h interaction with the nanoparticles. Each control group and test group had 5 replicates, and for each replicate, scoring was carried out for 1000 cells. The mitotic index of the control root tips was found to be 41.8±2.0 %, and there were no signs of chromosomal aberrations. After the exposure to Al_2O_3 NPs at 0.01-, 0.1-, 1-, 10-, and 100-μg/mL concentrations, a dose-dependent decrease in the percentages of mitotic index was observed in the treated group in comparison to the control cells. Table 3 represents the clastogenic effects of Al_2O_3 NPs on the chromosomes of *A. cepa*. A variety of different chromosomal aberrations (CA) were observed in the root tip cells after their interaction with Al_2O_3 NPs.

The different mitotic phases, namely, interphase, prophase, metaphase, anaphase, and telophase, were observed in the control *A. cepa* root cells. Upon exposure to various concentrations of NPs, different features like chromosomal stickiness, chromosomal breaks, laggard and clumped chromosomes, multipolar anaphase, and disturbed metaphase and anaphase were observed. At a very low concentration of 0.01 μg/mL of Al_2O_3 NPs, there were occurrences of chromosomal aberrations like clumped chromosomes, sticky metaphase, and chromosomal breaks (Fig. 1a1–a3). At 0.1-μg/mL concentration, there was presence of sticky

Table 2 Mitotic index of *A. cepa* root cells treated with different concentration of Al_2O_3 NPs

Treatment of NP	Sample (N=5)	MI %	P %	M %	A %	T %	Mean(MI%)±SE
Control (DI water)	Sample 1	41.7	88.1	4.8	2.0	4.8	41.8±2.0
	Sample 2	43.5	89.4	3.9	1.7	4.8	
	Sample 3	40.4	88.8	3.9	2.7	4.4	
	Sample 4	38.9	90.4	4.2	1.4	3.9	
	Sample 5	44.5	89.3	4	2.2	4.2	
0.01 μg/mL	Sample 1	39.9	89.1	5.1	1.6	4.0	40.9±0.9
	Sample 2	40.8	85.7	2.9	1.6	1.9	
	Sample 3	40.9	84.9	2.4	2.1	4.3	
	Sample 4	40.5	84.2	3.9	2.9	2.9	
	Sample 5	42.6	88.9	4	2.8	4.5	
0.1 μg/mL	Sample 1	37.6	92.8	2.8	1.2	3.0	35.4±1.2
	Sample 2	36.0	85.6	2.6	2.9	2.6	
	Sample 3	34.4	92.4	2.0	2.9	2.6	
	Sample 4	34.2	90.6	3.6	3.9	1.8	
	Sample 5	34.9	93.0	2.4	2.4	2.0	
1 μg/mL	Sample 1	34.5	92.9	2.9	2.0	2.0	33.9±0.4
	Sample 2	33.9	92.4	3.1	3.1	1.7	
	Sample 3	33.4	95.2	2.0	1.1	1.4	
	Sample 4	34.4	95.0	1.6	1.3	1.9	
	Sample 5	34.6	93.6	2.0	2.0	2.0	
10 μg/mL	Sample 1	32.4	94.8	1.7	1.3	2.0	31.8±0.5
	Sample 2	31.0	94.0	2.3	1.6	1.9	
	Sample 3	31.9	93.8	2.2	1.9	1.9	
	Sample 4	32.4	95.6	1.5	1.2	1.5	
	Sample 5	31.5	95.3	1.8	1.5	1.2	
100 μg/mL	Sample 1	31.0	95.2	1.7	1.7	1.3	28.6±1.3
	Sample 2	29.4	96.5	1.3	1.0	1.0	
	Sample 3	28.9	96.1	1.7	1.0	1.0	
	Sample 4	27.3	96.8	0.6	1.0	1.3	
	Sample 5	27.3	96.6	1.1	1.1	1.1	

1000 number of cells were scored per test concentration

metaphase, disturbed metaphase, and clumped chromosomes (Fig. 1b1–b2). Similarly, sticky metaphase, disturbed metaphase and anaphase, chromosomal breaks, and clumped chromosomes (Fig. 1c1–c4) were observed at 1-μg/mL Al_2O_3 NP concentration.

At 10 μg/mL, the chromosomal aberrations observed were chromosomal breaks and sticky metaphase (Fig. 1d1–d2). Similarly, at a high concentration of 100 μg/mL, there were sticky metaphase, clumped chromosomes, diagonal anaphase, and diagonal and multipolar anaphase (Fig. 1e1–e4).

Table 3 Percentage of chromosomal aberration observed in Al_2O_3-treated *A. cepa* root tip cells

Treatment	Chromosome break (%)	Sticky chromosome (%)	Laggard chromosome (%)	Clumped chromosome (%)	Chromosomal bridge (%)	Disturbed anaphase and metaphase (%)	Diagonal anaphase (%)	Multipolar anaphase (%)
Control (DI water)	0±0	0±0	0±0	0±0	0±0	0±0	0±0	0±0
0.01 μg/mL	0.03±0.2	0.04±0.1	0±0.1	0.042±0.1	0±0	0.039±0.2	0.3±0.2	0±0.1
0.1 μg/mL	0.037±0.1	0.20±0.1	0±0	0.03±0.1	0±0	0.005±0.2	0.44±0.1	0±0.1
1 μg/mL	0.34±0.2	0.02±0.1	0.45±0.2	0±0	0.54±0.1	0.47±0.2	0±0.2	0.1±0.1
10 μg/mL	0.67±0.2	0.05±0.2	0.10±0.1	0.05±0.2	0.69±0.1	0.39±0.1	0.58±0.2	1.12±0.1
100 μg/mL	1.23±0.1	2.44±0.1	3.09±0.1	0.7±0.3	2.48±0.1	1.8±0.3	2.30±0.3	2.0±0.2

1000 number of cells were scored per test concentration

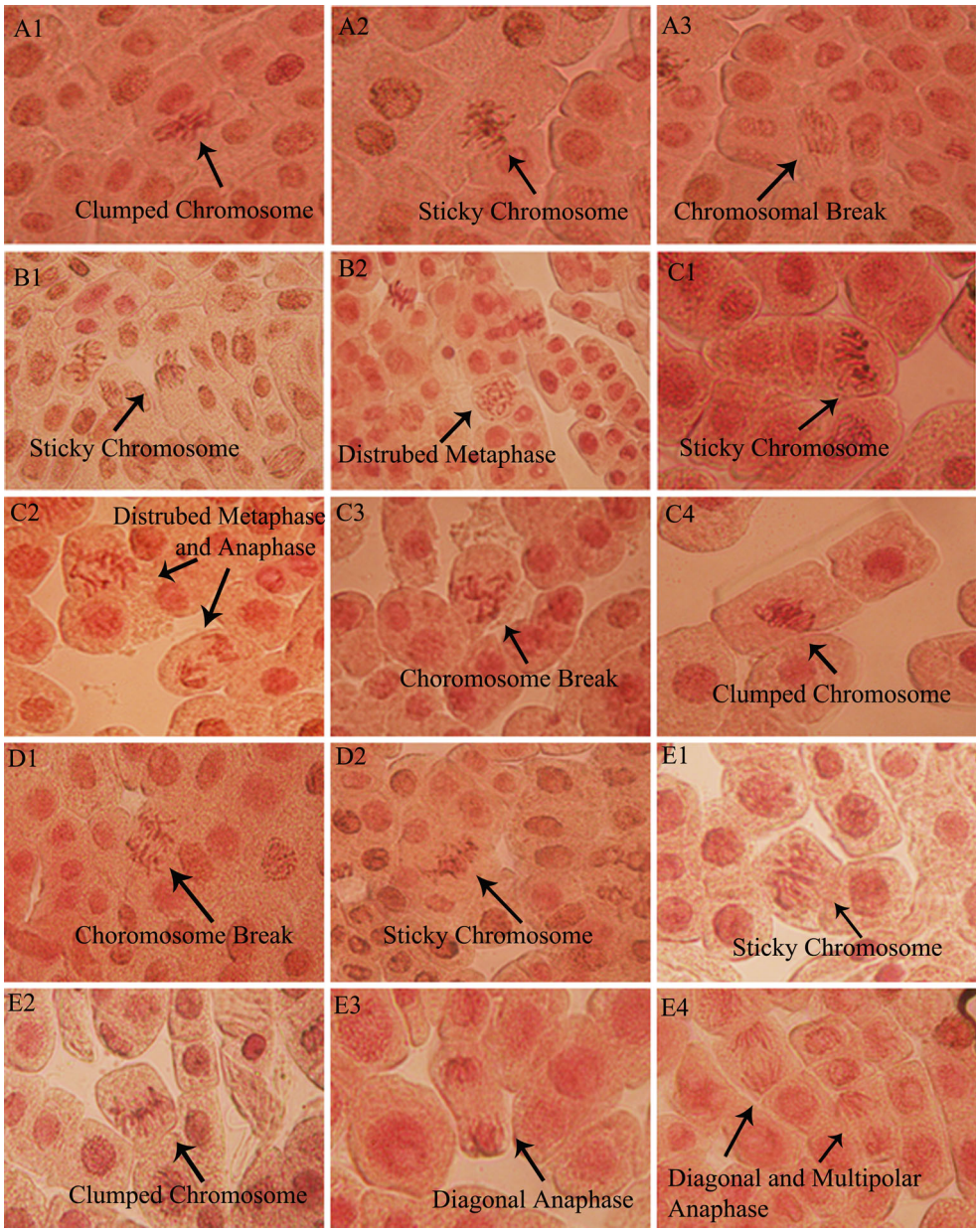

Fig. 1 Chromosomal aberrations observed under optical microscope: **a1**–**a3** the clumped chromosome, sticky chromosome, and chromosome break upon exposure to 0.01 μg/mL NPs; **b1**–**b2** the sticky metaphase and disturbed metaphase treated with 0.1 μg/mL of NPs; **c1**–**c4** the sticky metaphase, disturbed metaphase and anaphase, chromosomal break, and clumped chromosome treated with 1 μg/mL of NPs; **d1**–**d2** the chromosome break and sticky metaphase upon exposure to 10 μg/mL of NPs; **e1**–**e4** the sticky metaphase, clumped chromosome, diagonal anaphase, and diagonal and multipolar anaphase treated with 100 μg/mL of NPs

Fluorescence microscopy

The chromosomal aberrations in root tip cells of *A. cepa* after interaction with Al_2O_3 NPs (0.01 and 100 μg/mL) were observed under a fluorescence microscope at a magnification of ×1000 and analyzed in comparison to the control group. At a minimum exposure level of 0.01 μg/mL of Al_2O_3 NPs, characteristics like binucleate cells, clumped chromosomes, and diagonal anaphase were noticed. Similarly, there were occurrences of chromosomal bridges, multipolar anaphase, and sticky metaphase at a maximum concentration of 100 μg/mL of Al_2O_3 NPs (Fig. 2a1–a2).

Confocal laser scanning microscopy

The root tip cells of *A. cepa* before and after interaction with Al_2O_3 NPs were analyzed by confocal microscopy. Figure 2b, c shows the confocal microscopic images of various chromosomal aberrations observed at 0-, 0.01-, and 100-μg/mL concentrations of Al_2O_3 NPs under×1000 magnification. The formation of clumped chromosomes, nuclear blebbing, and binucleate cells was observed upon the exposure to 0.01 μg/mL of Al_2O_3 NP concentration. Sticky metaphase and binucleate cells were also observed, but only at a higher frequency of 100 μg/mL of Al_2O_3 NP concentration. These images obtained with the aid of fluorescence

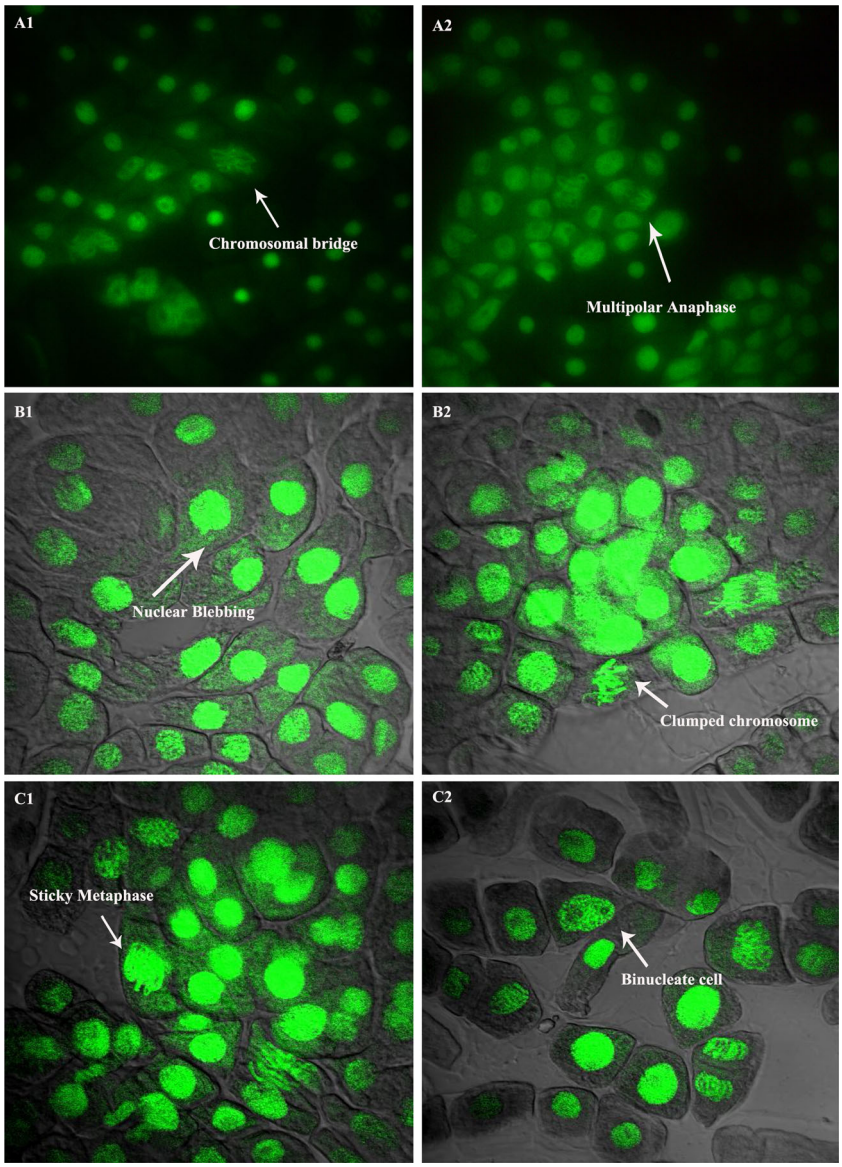

Fig. 2 Photo micrograph of chromosomal aberrations: **a1**–**a2** the chromosomal bridge and multipolar anaphase after exposure to 100 μg/mL of NPs under the fluorescence microscope; **b1**–**b2** nuclear blebbing and clumped chromosome; and **c1**–**c2** the sticky metaphase and binucleate cell formation after exposure to 0.01 and 100 μg/mL of NPs under confocal laser scanning microscope

imaging provided the clearest observation of chromosomal aberrations.

The decrease in MI from 42 to 28 % in a dose-dependent manner and the stimulation of chromosomal aberration upon the exposure to NPs suggested that the NPs were capable of increasing the DNA damages in root tip cells. The reduction in the mitotic index was due to the blockage at G1 stage, thereby suppressing the DNA synthesis (Mohandas and Grant 1972). The improper folding of chromosomes and inhibition of spindle fiber formation leads to the formation of sticky chromosomes. The occurrence of disturbed metaphase was mainly due to the disturbance in spindle fiber apparatus (Darlington and Mc Leish 1951). The other significant chromosomal aberrations observed during both metaphase and anaphase were due to the depolymerization of spindle fibers as a result of shifting of poles (Mederios and Takahashi 1987).

The genotoxicity study carried out by Pakrashi et al. (2014) strongly suggested that the exposure of *A. cepa* root tips to TiO_2 NPs at both lower (12.5 μg/mL) and higher concentrations (100 μg/mL) gave rise to various chromosomal aberrations, and there was a considerable decrease in the mitotic index in a dose-dependent manner, which was similar to our study. The reports on the cytotoxic and genotoxic potentials of ZnO NPs and AgNPs in *A. cepa* have also shown the concentration-dependent inhibition of mitotic index (Kumari et al. 2009, 2011). Through the toxicity evaluation of cobalt and zinc oxide nanoparticles by Ghodake et al. (2011), it can be implied that the accumulation of NPs within the cells and chromosomes resulted in the retardment of the root elongation.

By summarizing the microscopic examinations and correlating them with previous works, it can be found that the

cytogenetic potential of Al_2O_3 NPs was remarkably significant in the studied concentration range.

Biouptake of NPs

The biouptake potential is assumed to be an important parameter to evaluate the toxicity of nanoparticles. The ICP-OES analysis was performed to quantify the amount of aluminum ions internalized into the *A. cepa* root cells. The concentrations of Al ions that were internalized into the *A. cepa* root tip cells upon the exposure to various NP concentrations (0.1, 1, 10, and 100 μg/mL) are shown in Table 4. The internalized concentration for 0.01 μg/mL of NPs was assumed to be negligible as the concentration was below the detection limit of the instrument. The elemental analysis showed a concentration-dependent increase in the internalization of metal ions into the root cells.

Asztemborska et al. (2015) have suggested that the accumulation of Al_2O_3 NPs in the plant cells and their transport within the system increase with increasing concentrations of NPs. Pakrashi et al. (2014) have reported that the internalization or uptake of NPs contribute a major role in the toxic effect toward *A. cepa* by generating oxidative stress in the cells. Similarly, reports were found that the internalization of Ag and ZnO NPs into the *A. cepa* root cells can have negative effects and lead to DNA damage (Kumari et al. 2009, 2011). Thus, these results indicate that the internalization of NPs into the root cells can attribute toward the toxicity in cells, which can be correlated with the decrease in the mitotic index observed through the microscopic analyses.

Superoxide dismutase assay

The SOD assay has been performed to confirm the oxidative stress induced by Al_2O_3 NPs in the *A. cepa* root tip cells. The concentrations of NPs for the SOD assay have been selected based on the results obtained from the internalization/uptake studies. Insignificant differences were observed in the biouptake between 0.1 and 1 μg/mL and also between 1- and 10-μg/mL concentrations. Therefore, the minimum (0.01 μg/mL), maximum (100 μg/mL), and intermediate (1 μg/mL) concentrations of NPs have been considered for SOD analysis. Table 5 shows the oxidative stress profile in *A. cepa* root tips upon exposure to Al_2O_3 NPs. At 0.01-, 1-, and 100-μg/mL concentrations of Al_2O_3 NPs, the SOD % were found to be 8.3±0.02, 35.4±0.005, and 75.00±0.02 %, respectively ($p<0.05$). The SOD activity was found to have increased on increasing the concentrations of Al_2O_3 NPs, and a maximum increase was found at 100 μg/mL of NPs. The SOD analysis showed a concentration-dependent generation of intracellular oxidative species on increasing the concentration of Al_2O_3 NPs. The increase in SOD % shows the impact of Al_2O_3 NPs with regard to oxidative stress generation in *A. cepa* root tips, which suggested the toxicity of Al_2O_3 NPs on the root tips of *A. cepa*.

The NPs are capable of entering through cell membrane, and their accumulation in the cytoplasm may lead to various toxic effects in the form of mitochondrial dysfunction, oxidative stress, and cell death (Kim et al. 2009). The genotoxicity of Al may occur due to the modification of chromatin structure, induction of ROS, or liberation of DNase from the lysosomes (Banasik et al. 2005). Anane and Creppy (2001) and Rao and Stein (2003) have reported that the formation of ROS can result due to the interaction of Al with the cells. The leached out Al^{3+} ions and the surface charge-based interaction

Table 4 Quantification of internalized of Al ions into the *A. cepa* root tips by ICP-OES

Concentration of Al_2O_3 NPs (μg/mL)	Internalized Al ions (%)
0.01	BDL
0.1	3.58±0.02
1	4.10±0.00
10	5.68±0.30
100	38.50±18.00

BDL below detection limit

Table 5 Relative antioxidant enzyme (SOD) production in percentage by *A. cepa* root tip cells upon its exposure to various concentrations of Al_2O_3 NPs

Concentration of Al_2O_3 NPs (μg/mL)	SOD (%)
0.01	8.30±0.02
1	35.40±0.00
100	75.00±0.02

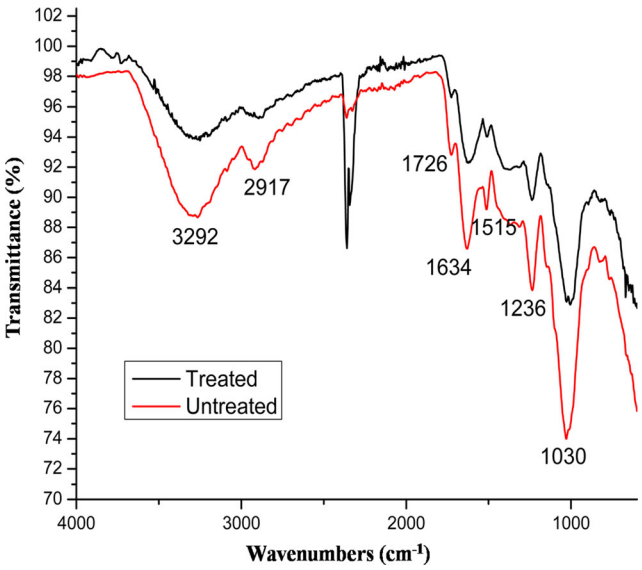

Fig. 3 FT-IR spectra of *A. cepa* root tip before and after interaction with Al_2O_3 NPs

of Al_2O_3 NPs may also synergistically modify the surface functional moieties, which thereby result in oxidative stress and cell membrane damage due to the triggering of several signal transduction cascades (Pakrashi et al. 2013). Tang et al. (2007) have suggested that the increase in the ROS level may thus stimulate the production of the antioxidative enzyme, SOD. Therefore, the increased activity of antioxidant enzymes like superoxide dismutase in treated root tip cells as compared to the control reflected that these enzymes were involved in countering the excessive ROS generated during the stress induced by NPs.

FT-IR analysis

Surface chemical characterizations of *A. cepa* root cells before and after interaction with nanoparticles have been analyzed and shown in Fig. 3. The FT-IR spectra of control root tip cells were around the range 4000–900 cm^{-1}, which revealed the presence of biochemical components like carbohydrates, proteins, and lipid moieties in root cells (Lu et al. 2011). The peak at 3292 cm^{-1} was due to N–H stretching of protein and O–H stretching of carbohydrates and water, while the peaks at 2917 and 1726 cm^{-1} were due to the C–H stretching of methyl group and C=O vibration of lipids (Lu and Rasco 2012). The peaks positioned at 1634 and 1515 cm^{-1} indicated the presence of amide I and amide II groups (Maquelin et al. 2002). The peak at 1236 cm^{-1} was assigned to the asymmetric and symmetric P=O stretching modes of nucleic acids, while the band at 1030 cm^{-1} was due to the glycogen and CH_2OH vibration (Movasaghi et al. 2008).

Slight peak shifts around the carbohydrate, lipid, and amide regions were observed in the NP-treated root samples. In addition, the bands at 1236 and 1030 cm^{-1} were shifted to 1234 and 1008 cm^{-1}, which clearly indicates the damage in DNA. The changes in the peak position and a decrease in the absorbance of the respective peaks were observed in treated sample as compared to the control, which illustrated the impact of NPs on the chemical structures of the various components in the cells. Thus, the FT-IR analysis revealed that the adsorption of NPs onto the surface of root tip could induce the breakage of cell membrane, and their internalization may cause DNA damage.

Conclusion

The present study demonstrated the dose-dependent cytogenetic effects of the Al_2O_3 NPs toward the *A. cepa* in a wide range of exposure concentration from 0.01 to 100 μg/mL. The increase in various chromosomal aberrations and decrease in mitotic index as a function of Al_2O_3 NP concentrations were confirmed by the microscopic studies. The concentration-dependent uptake/internalization profiles of the Al_2O_3 NPs have been substantiated by ICP-OES. In order to counteract the ROS produced by Al_2O_3 NPs, an increased level of SOD activity was observed proportional to the nanoparticle concentration. Thus, the *A. cepa* assay can be employed as a bioindicator for the successful evaluation of cytogenetic effects of Al_2O_3 NPs in plant systems.

Acknowledgments We would like to thank the Sophisticated Analytical Instrument Facility (SAIF) at Indian Institute of Technology, Madras for the ICP-OES analysis facility and Indian Institute of Sciences, Bangalore for the Confocal Laser microscopy facility.

Compliance with Ethical Standards There were no human participants nor animals involved in this study.

Conflict of interest The authors declare that they have no conflict of interests.

References

Anane R, Creppy EE (2001) Lipid peroxidation as pathway of aluminium cytotoxicity in human skin fibroblast cultures: prevention by superoxide dismutase catalase and vitamins E and C. Hum Exp Toxicol 20:477–481

Arruebo M, Valladares M, González-Fernández Á (2009) Antibody-conjugated nanoparticles for biomedical applications. J Nanomater 2009:1–24

Asztemborska M, Steborowski R, Kowalska J, Bystrzejewska-Piotrowska G (2015) Accumulation of Aluminium by Plants Exposed to Nano-and Microsized Particles of Al. Int J Environ Res 9(1):109–116

Bakare AA, Mosuro AA, Osibanjo O (2000) Effect of simulated leachate on chromosomes and mitosis in roots of *Allium cepa* (L). J Environ Biol 21(3):263–271

Baker TJ, Tyler CR, Galloway TS (2014) Impacts of metal and metal oxide nanoparticles on marine organisms. Environ Pollut 186:257–271

Banasik A, Lankoff A, Piskulak A, Adamowska K, Lisowska H, Wojcik A (2005) Aluminium-induced micronuclei and apoptosis in human peripheral blood lymphocytes treated during different phases of the cell cycle. Environ Toxicol 20:402–406

Cabrera GL, Rodriguez DMG (1999) Genotoxicity of soil from farmland irrigated with wastewater using three plant bioassays. Mutat Res Fundam Mol Mech 426(2):211–214

Chen L, Yokel RA, Hennig B, Toborek M (2008) Manufactured aluminum oxide nanoparticles decrease expression of tight junction proteins in brain vasculature. J Neuroimmune Pharmacol 3(4):286–295

Chen R, Ratnikova TA, Stone MB, Lin S, Lard M, Huang G, Hudson JS, Ke PC (2010) Differential uptake of carbon nanoparticles by plant and mammalian cells. Small 6(5):612–617

Darlington CD, Mc Leish L (1951) Action of maleic hydrazide on the cell. Nature 167:407–408

Darlington TK, Neigh AM, Spencer MT, Nguyen OT, Oldenburg SJ (2009) Nanoparticle characteristics affecting environmental fate and transport through soil. J Environ Toxicol Chem 28(6):1191–1199

Di Virgilio AL, Reigosa M, Arnal PM, Lorenzo F, de Mele M (2010) Comparative study of the cytotoxic and genotoxic effects of titanium oxide and aluminium oxide nanoparticles in Chinese hamster ovary (CHO-K1) cells. J Hazard Mater 177(1):711–718

Donaldson K, Stone V, Clouter A, Renwick L, MacNee W (2001) Ultrafine particles. Occup Environ Med 58(3):211–216

Faraji AH, Wipf P (2009) Nanoparticles in cellular drug delivery. Bioorg Med Chem 17(8):2950–2962

Firbas P, Amon T (2013) Allium Chromosome Aberration Test for Evaluation Effect of Cleaning Municipal Water with Constructed Wetland (CW) in Sveti Tomaž, Slovenia. J Bioremed Biodegrad 4(4):189–193

Fiskesjo G (1985) The Allium test as a standard in environmental monitoring. Hereditas 102:99–112

Fiskesjo G (1997) Allium test for screening chemicals; evaluation of cytological parameters. In: Wuncheng W, Gorsuch JW, Hughes JS (eds) Plants for environmental studies. CRC Lewis Publishers, Boca Raton, pp 307–333

Future Markets Inc. (2013) The global market for metal oxide nanoparticles to 2020, 322. Available: http://www.researchandmarkets.com/research/jkjd5k/the_global_market

Ghodake G, Seo YD, Lee DS (2011) Hazardous phytotoxic nature of cobalt and zinc oxide nanoparticles assessed using *Allium cepa*. J Hazard Mater 186(1):952–955

Grant WF (1982) Chromosome aberration assays in Allium: A report of the US Environmental Protection Agency gene-tox program. Mutat Res Rev Genet 99(3):273–291

Hasenstein KH, Evans ML (1988) Effects of cations on hormone transport in primary roots of *Zea mays*. Plant Physiol 86(3):890–894

Illéš P, Schlicht M, Pavlovkin J, Lichtscheidl I, Baluška F, Ovečka M (2006) Aluminium toxicity in plants: internalization of aluminium into cells of the transition zone in Arabidopsis root apices related to changes in plasma membrane potential, endosomal behaviour, and nitric oxide production. J Exp Bot 57(15):4201–4213

Jiang J, Oberdörster G, Biswas P (2009) Characterization of size, surface chargeagglomeration state of nanoparticle dispersion for toxicological studies. J Nanoparticle Res 11:77–89

Kanaya N, Gill BS, Grover IS, Murin A, Osiecka R, Sandhu SS, Andersson HC (1994) *Vicia faba* chromosomal aberration assay. Mutat Res Fundam Mol Mech 310(2):231–247

Kim YJ, Choi HS, Song MK, Youk DY, Kim JH, Ryu JC (2009) Genotoxicity of aluminum oxide (Al_2O_3) nanoparticle in mammalian cell lines. Mol Cell Toxicol 5(2):172–178

Kristen U (1997) Use of higher plants as screens for toxicity assessment. Toxicol in Vitro 11(1):181–191

Kumari M, Mukherjee A, Chandrasekaran N (2009) Genotoxicity of silver nanoparticles in *Allium cepa*. Sci Total Environ 407(19): 5243–5246

Kumari M, Khan SS, Pakrashi S, Mukherjee A, Chandrasekaran N (2011) Cytogenetic and genotoxic effects of zinc oxide nanoparticles on root cells of *Allium cepa*. J Hazard Mater 190(1):613–621

Liman R (2013) Genotoxic effects of Bismuth (III) oxide nanoparticles by Allium and Comet assay. Chemosphere 93(2):269–273

Lu X, Rasco B (2012) Determination of Antioxidant Content and Antioxidant Activity in Foods using Infrared Spectroscopy and Chemometrics: A Review. Crit Rev Food Sci Nutr 52(10):853–875

Lu X, Rasco BA, Jabal JM, Aston DE, Lin M, Konkel ME (2011) Investigating antibacterial effects of garlic (*Allium sativum*) concentrate and garlic-derived organosulfur compounds on *Campylobacter jejuni* by using Fourier transform infrared spectroscopy, Raman spectroscopy, and electron microscopy. Appl Environ Microbiol 77(15):5257–5269

Maquelin K, Kirschner C, Choo-Smith LP, Van Den Braak N, Endtz HP, Naumann D, Puppels GJ (2002) Identification of medically relevant microorganisms by vibrational spectroscopy. J Microbiol Methods 51:255–271

Mederios MDC, Takahashi CS (1987) Effects of *Luffa operculata* on *Allium cepa* root tips cell. Cytologia 52:255–259

Mohandas T, Grant WF (1972) Cytogenetic effect of 2, 4-D and amitol in relation to nuclear volume DNA content in some higher plants. Can J Genet Cytol 14:773–783

Movasaghi Z, Rehman S, Rehman IU (2008) Fourier transform infrared (FTIR) spectroscopy of biological tissues. Appl Spectrosc Rev 43: 134–179

Mukherjee A, Mohammed Sadiq I, Prathna TC, Chandrasekaran N (2011) Antimicrobial activity of aluminium oxide nanoparticles for potential clinical applications. In: Méndez-Vilas A (ed) Science against microbial pathogens: communicating current research and technological advances. Spain. vol. 1, pp 245–251

Pakrashi S, Dalai S, Prathna TC, Trivedi S, Myneni R, Raichur AM, Chandrasekaran N, Mukherjee A (2013) Cytotoxicity of aluminium oxide nanoparticles towards fresh water algal isolate at low exposure concentrations. Aquat Toxicol 132:34–45

Pakrashi S, Jain N, Dalai S, Jayakumar J, Chandrasekaran PT, Raichur AM, Chandrasekaran N, Mukherjee A (2014) In Vivo Genotoxicity Assessment of Titanium Dioxide Nanoparticles by Allium cepa Root Tip Assay at High Exposure Concentrations. PLoS One 9(2): e87789

Panda KK, Achary VMM, Krishnaveni R, Padhi BK, Sarangi SN, Sahu SN, Panda BB (2011) *In vitro* biosynthesis and genotoxicity bioassay of silver nanoparticles using plants. Toxicol in Vitro 25(5): 1097–1105

Prabhakar PV, Reddy UA, Singh SP, Balasubramanyam A, Rahman MF, Indu Kumari S, Agawane SB, Murty USN, Grover P, Mahboob M (2012) Oxidative stress induced by aluminium oxide nanomaterials after acute oral treatment in Wistar rats. J Appl Toxicol 32:436–445

Rao KSJ, Stein R (2003) First evidence on induced topological changes in supercoiled DNA by an aluminium Daspartate complex. J Biol Inorg Chem 8:823–830

Rico CM, Majumdar S, Duarte-Gardea M, Peralta-Videa JR, Gardea-Torresdey JL (2011) Interaction of nanoparticles with edible plants and their possible implications in the food chain. J Agric Food Chem 59(8):3485–3498

Ryan PR, Ditomaso JM, Kochian LV (1993) Aluminium toxicity in roots: an investigation of spatial sensitivity and the role of the root cap. J Exp Bot 44(2):437–446

Sadiq IM, Pakrashi S, Chandrasekaran N, Mukherjee A (2011) Studies on toxicity of aluminum oxide (Al_2O_3) nanoparticles to microalgae species: *Scenedesmus sp*. and *Chlorella sp*. J Nanoparticle Res 13(8):3287–3299

Satapathy R, Swamy P (2013) Preparative isolation of flavonoids from wattakaka volubilis (linn. f.) leaf extracts and its role as antimitotic and antiproliferating agent. Int J Pharm Biol Sci 4(3):454–460

Sayes CM, Warheit DB (2009) Characterization of nanomaterials for toxicity assessment. Wiley Interdiscip Rev Nanomed Nanobiotechnol 1(6):660–670

Schrand AM, Rahman MF, Hussain SM, Schlager JJ, Smith DA, Syed AF (2010) Metal-based nanoparticles and their toxicity assessment. J Nanomed Nanobiotechnol 2:544–568

Tang D, Shi S, Li D, Hu C, Liu Y (2007) Physiological and biochemical responses of *Scytonema javanicum* (cyanobacterium) to salt stress. J Arid Environ 71(3):312–320

Tsaousi A, Jones E, Case CP (2010) The *in vitro* genotoxicity of orthopaedic ceramic (Al_2O_3) and metal (CoCr alloy) particles. Mutat Res Genet Toxicol Environ 697(1):1–9

World Health Organization (1985) Guide to short-term tests for detecting mutagenic and carcinogenic chemicals. Environmental Health Criteria 51. WHO, Geneva, p 107

Yang ST, Wang T, Dong E, Chen XX, Xiang K, Liu JH, Liu YF, Wang H (2012) Bioavailability and preliminary toxicity evaluations of alumina nanoparticles in vivo after oral exposure. Toxicol Res 1(1):69–74